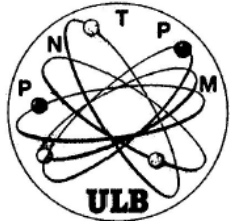


# Super heavy nuclei

Status and difficulties of self-consistent mean-field approaches

# Status and prospect for SHE

- Several studies in the last 10 years, self-consistent mean-field methods can be routinely applied to SHE.
- Short review of typical results
- Studies of very heavy nuclei = tests of models (interaction and method)?
- Main problems



# HFB methods

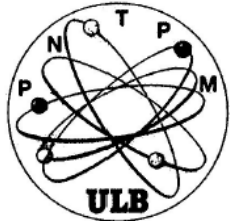
- Effective interaction for mean-field and pairing:

Minimization of the total energy  $\rightarrow$  HFB ground state  $|\Phi\rangle$

$$E = \langle \Psi | \hat{H} | \Psi \rangle = E[\rho, \kappa, \kappa^*]$$

with constraints on  $N$  and  $Z$   $\langle \Psi | \hat{N}_q | \Psi \rangle = N_q$ .

Solution of the HFB equations on a 3-dimensional mesh  
(triaxiality included)



Minimization of  $E^\lambda = E - \lambda_q \langle \Psi | \hat{N}_q | \Psi \rangle$  in a basis

$$\mathcal{H} \begin{pmatrix} U_n \\ V_n \end{pmatrix} = e_n \begin{pmatrix} U_n \\ V_n \end{pmatrix},$$

$$\mathcal{H} = \begin{pmatrix} h - \lambda & \Delta \\ -\Delta^* & -h^* + \lambda \end{pmatrix},$$

$U$  and  $V$  are transformation matrices

$e_n$  are the quasi particle energies

Great similarities between Skyrme, RMF and Gogny studies.

Same kind of successes, and of problems.

Main reference for this talk:

S.Cwiok , PHH and W. Nazarewicz PRL 83 1108 1999

Nature 433 705 2005

P. Bonche, M.Bender and PHH PRC 70 54304 2004

A.Afanasjiev et al. J. Phys.: Conf. Ser. 312 092004 2011

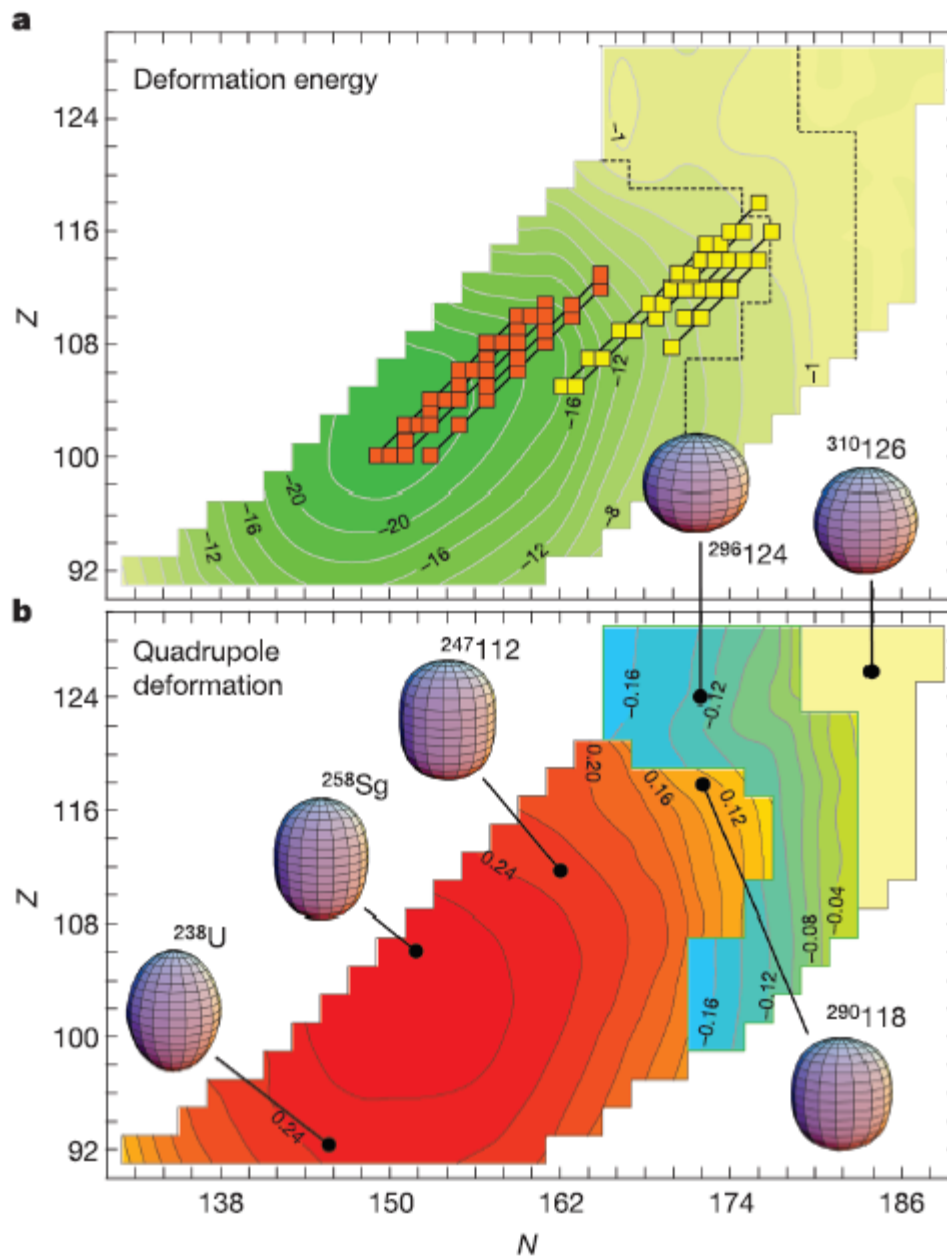
M. Bender et al. Phys. Rev C 60 034304 1999

A. Sobiczewski and K. Pomorski, Prog in Part. Nucl. Phys. 58 292 2007

Collaboration also with V. Hellemans and K. Washiama

# Skyrme HFB

## Deformation properties of super-heavies



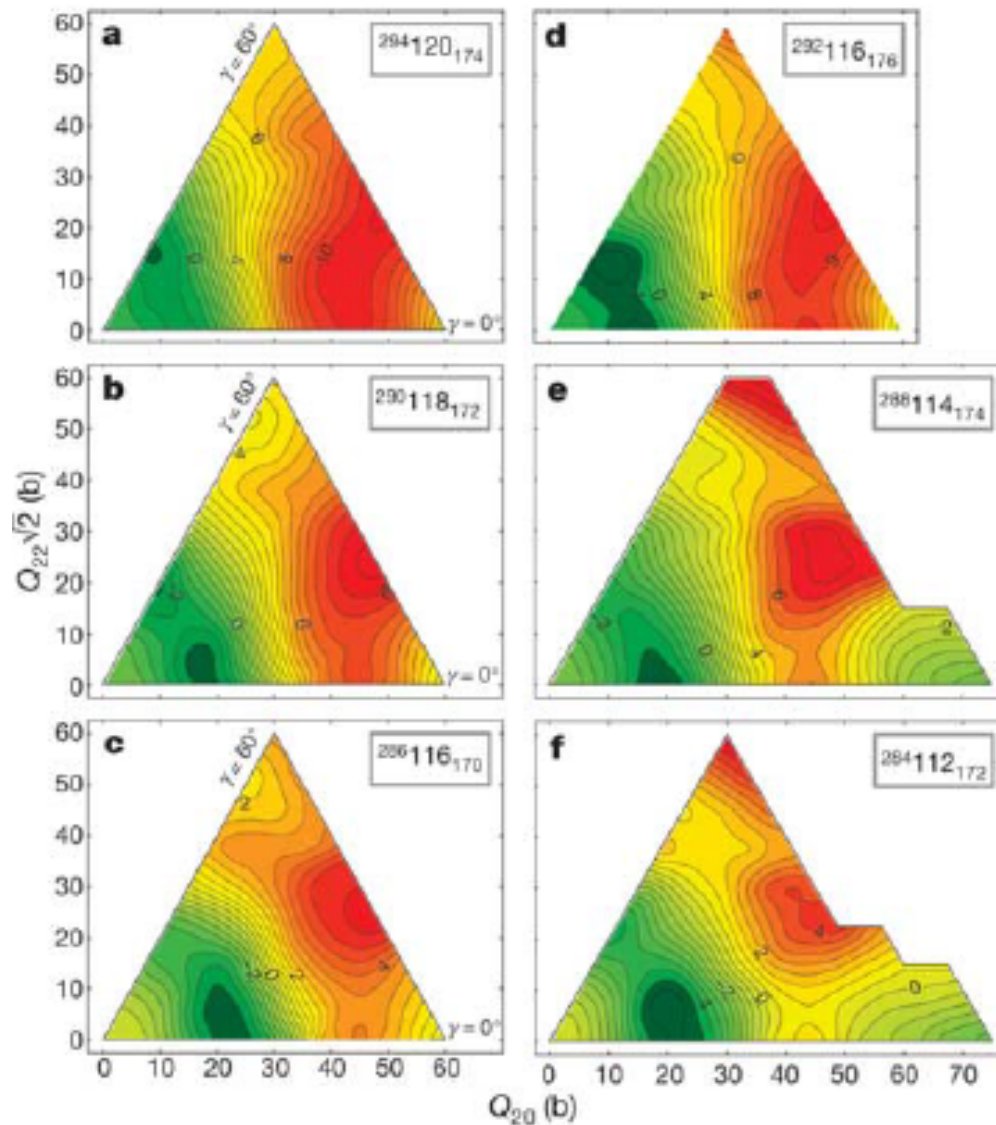


**Figure 3** Potential energy surfaces of the members of the  $\alpha$ -decay chains of  $^{294}_{120}$  (a–c) and  $^{292}_{116}$  (d–f) in the  $(Q_{20}, Q_{22})$  plane calculated with the SLy4 energy density functional. It is seen that both  $\alpha$ -decay sequences are associated with transition from oblate (or triaxial shapes) in the parent nuclei to prolate shapes in lighter daughter nuclei. The difference between contour lines is 0.5 MeV.

Microscopic calculations include automatically all the deformations that are not excluded by symmetry restrictions

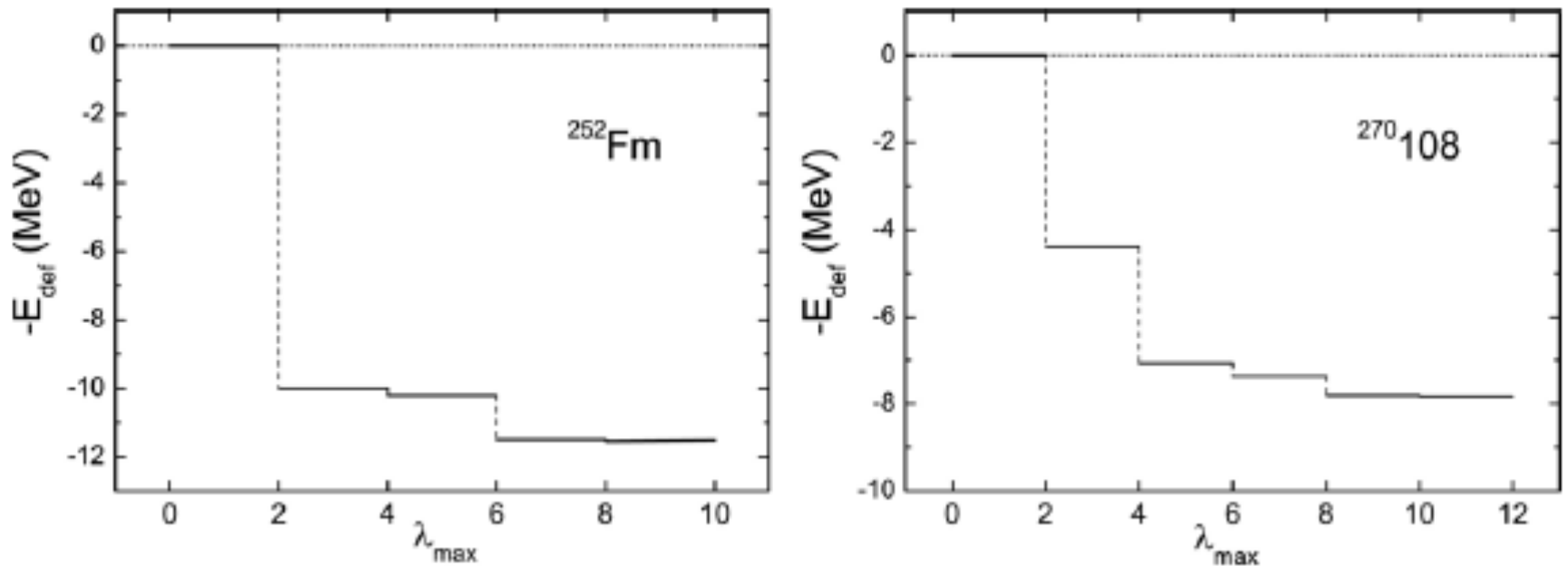
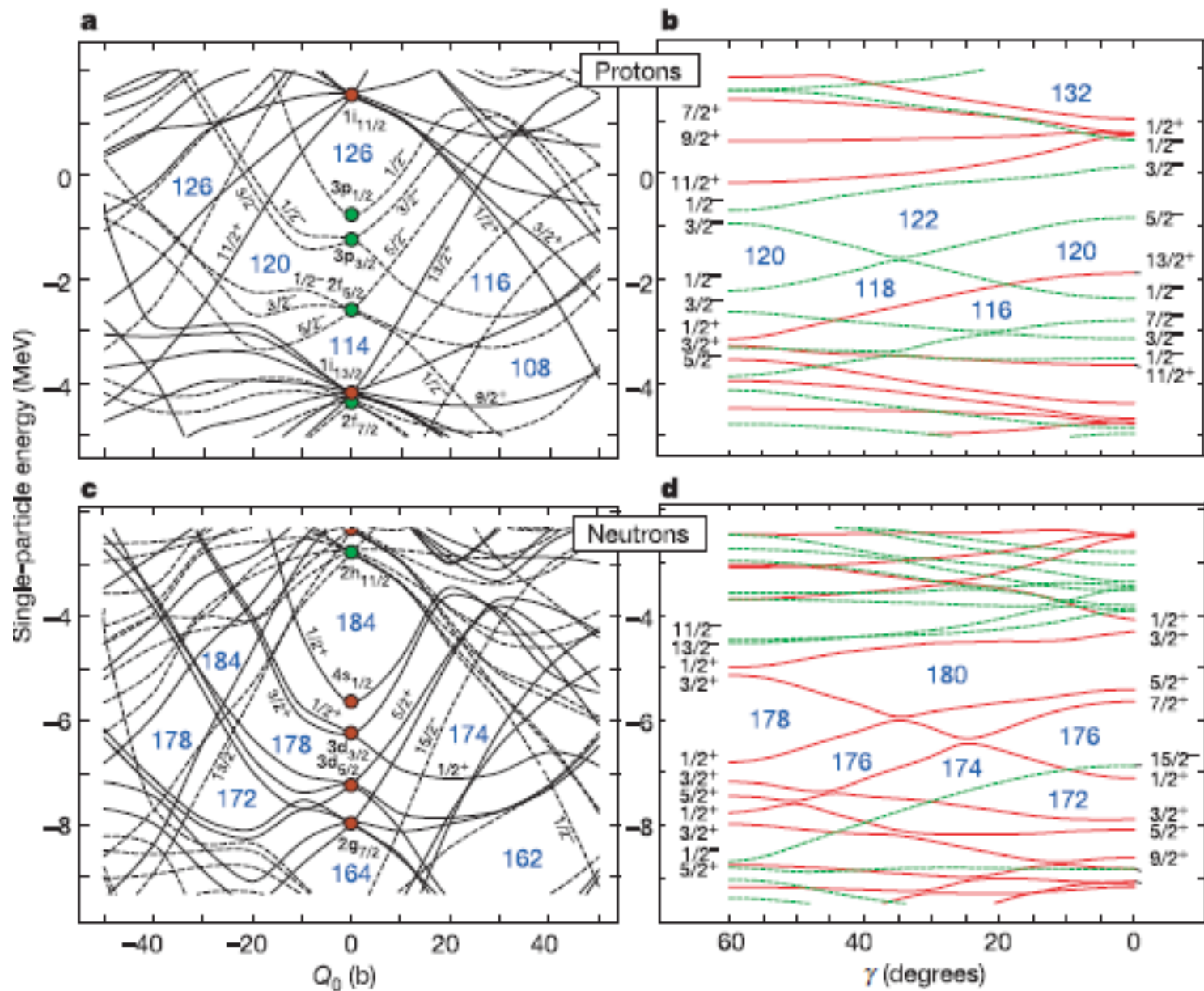


Fig. 9. Dependence of the deformation energy (taken with minus sign),  $-E_{\text{def}}$ , on  $\lambda_{\text{max}}$  for the nucleus  $^{252}\text{Fm}$  (l.h.s) and  $^{270}\text{Hs}$  (r.h.s.) [65].





# Beyond ground state properties of even-even nuclei

Breaking of time reversal invariance  
by a cranking constraint:

$$H' = H - \omega J_x \quad \text{rotational bands for deformed nuclei}$$

by quasi particle excitations:

Odd nuclei : 1 qp states:

$$\beta_i^\dagger |0\rangle$$

Even nuclei: 2qp states

Still a mean-field method

Full self-consistency for mean-field and pairing

No direct relation with the single-particle spectrum.

One does not have:  $E_{qp,i} = ((\epsilon_i - \lambda)^2 + \Delta^2)^{1/2}$

How to test the models?

How reliable are the models for nuclei just below the SHE?

Tests on: deformation properties (and fission barriers)  
moment of inertia of rotational bands  
spectra of odd nuclei  
2qp isomers in even nuclei

Nucleus	Orbital	Energy (MeV)	$\beta_2$
$^{293}_{116}$	$[604] \frac{7}{2}^+$	0	0.09
(10.47)	$[602] \frac{5}{2}^+$	0.31	0.09
	$[611] \frac{1}{2}^+$	0.52	0.08
	$[707] \frac{15}{2}^-$	0.93	0.09
$^{289}_{114}$	$[707] \frac{15}{2}^-$	0	0.12
(9.64)	$[611] \frac{1}{2}^+$	0.52	0.11
	$[604] \frac{7}{2}^+$	0.79	0.13
	$[602] \frac{5}{2}^+$	1.17	0.12
$^{285}_{112}$	$[611] \frac{1}{2}^+$	0	0.14
(8.88)	$[611] \frac{3}{2}^+$	0.60	0.14
	$[707] \frac{15}{2}^-$	0.62	0.13
	$[606] \frac{11}{2}^+$	0.65	0.15
	$[604] \frac{9}{2}^+$	0.72	0.15
$^{281}_{110}$	$[604] \frac{9}{2}^+$	0	0.19
(9.32)	$[606] \frac{11}{2}^+$	0.07	0.19
	$[611] \frac{1}{2}^+$	0.12	0.18
	$[611] \frac{3}{2}^+$	0.59	0.17
	$[613] \frac{5}{2}^+$	0.65	0.17
	$[716] \frac{13}{2}^-$	0.94	0.17
$^{277}_{108}$	$[611] \frac{1}{2}^+$	0	0.21
	$[604] \frac{9}{2}^+$	0.04	0.20
	$[613] \frac{5}{2}^+$	0.31	0.21
	$[716] \frac{13}{2}^-$	0.36	0.21
	$[611] \frac{3}{2}^+$	0.38	0.20

Nucleus	Orbital	Energy (MeV)	$\beta_2$
$^{293}_{118}$	$[707] \frac{15}{2}^-$	0	0.11
(11.59)	$[611] \frac{1}{2}^+$	0.16	0.10
	$[602] \frac{5}{2}^+$	0.84	0.12
	$[604] \frac{7}{2}^+$	0.98	0.10
$^{289}_{116}$	$[611] \frac{1}{2}^+$	0	0.13
(10.18)	$[606] \frac{11}{2}^+$	0.62	0.14
	$[611] \frac{3}{2}^+$	0.66	0.13
	$[604] \frac{9}{2}^+$	0.69	0.14
	$[707] \frac{15}{2}^-$	0.72	0.13
$^{285}_{114}$	$[606] \frac{11}{2}^+$	0	0.16
(10.60)	$[611] \frac{1}{2}^+$	0.04	0.16
	$[611] \frac{3}{2}^+$	0.15	0.16
	$[604] \frac{9}{2}^+$	0.16	0.16
	$[613] \frac{5}{2}^+$	0.28	0.15
	$[716] \frac{13}{2}^-$	0.73	0.16
$^{281}_{112}$	$[611] \frac{1}{2}^+$	0	0.19
(10.85)	$[604] \frac{9}{2}^+$	0.07	0.19
	$[611] \frac{3}{2}^+$	0.37	0.19
	$[613] \frac{5}{2}^+$	0.41	0.19
	$[606] \frac{11}{2}^+$	0.42	0.19
	$[716] \frac{13}{2}^-$	0.51	0.19
$^{277}_{110}$	$[716] \frac{13}{2}^-$	0	0.22
(11.07)	$[613] \frac{5}{2}^+$	0.02	0.21
	$[611] \frac{3}{2}^+$	0.07	0.21
	$[611] \frac{1}{2}^+$	0.15	0.22
	$[604] \frac{9}{2}^+$	0.27	0.21
	$[606] \frac{11}{2}^+$	0.83	0.21

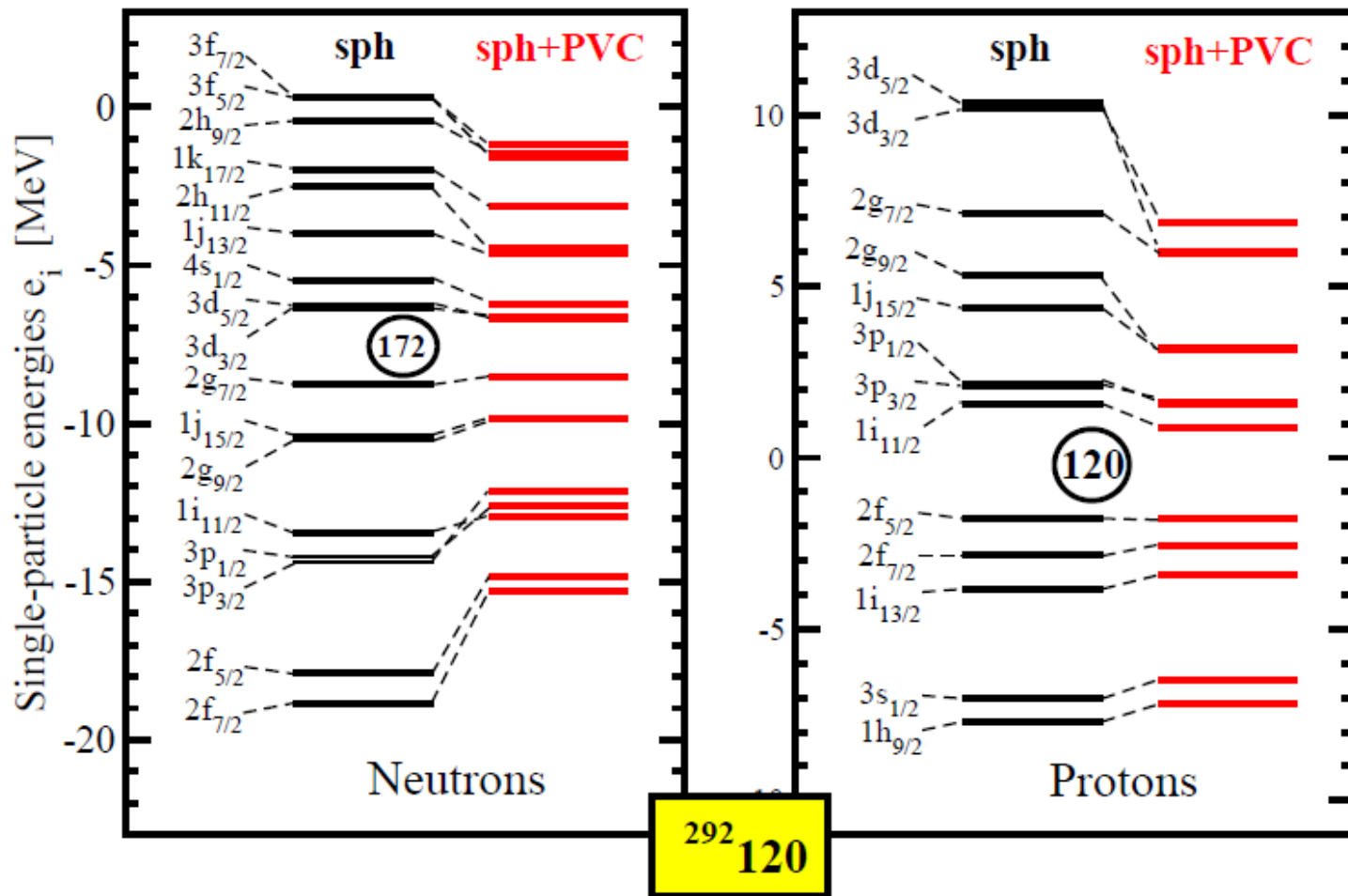


**Figure 3.** Neutron and proton single-particle states in the  $^{292}\text{120}$  nucleus. The left column each panel shows the spectra obtained in pure RMF calculations, while right column the spectra computed within RMF with allowance for the particle-vibration coupling. The calculations performed at spherical shape employing the NL3\* parameterization (from Ref. [15]).

A. Afanasjev, to be published (from J. Phys.: Conf. Ser. 312 092004 (2011))

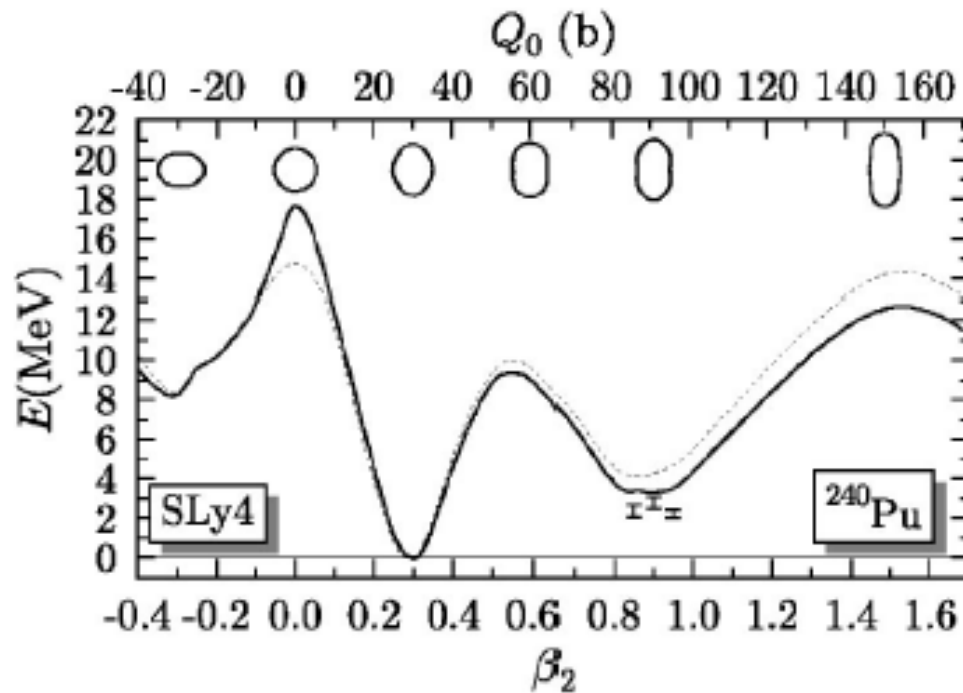
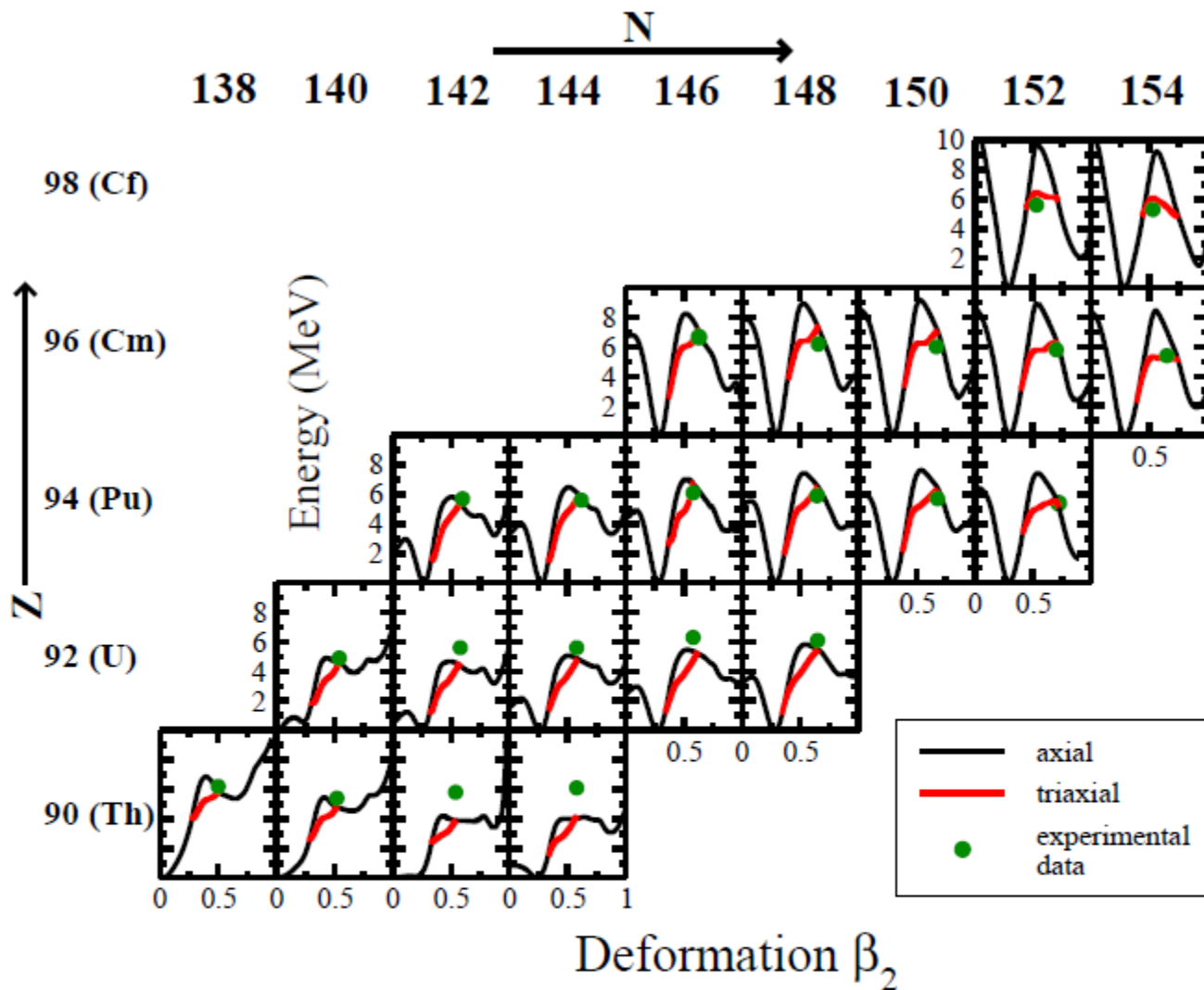
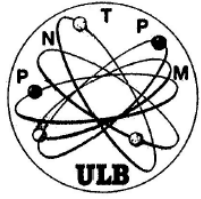


FIG. 1. Deformation energy curve of  $^{240}\text{Pu}$  obtained with SLy4 projected on  $N$  and  $Z$  (dashed line) and projected on  $N$ ,  $Z$ , and  $J=0$  (solid line). All energies are normalized to the deformed ground-state value of each curve. The available experimental data for the excitation energy of the superdeformed band head are shown at arbitrary deformation (see text). Shapes along the path are indicated by the density contours at  $\rho=0.07 \text{ fm}^{-3}$ .

Axial calculation, no octupoles but projection on  $N$ ,  $Z$  and  $J=0$   
 It decreases the excitation energy by around 3 MeV



**Figure 6.** Deformation energy curves of even-even actinide nuclei obtained in RMF+BCS calculations with the NL3\* parameterization. Experimental data are taken from Table IV in Ref. [42]. A typical uncertainty in the experimental values, as suggested by the differences among various compilations, is of the order of  $\pm 0.5$  MeV [42]. The deformation parameters  $\beta$  and  $\gamma$  are determined using the expressions  $\beta = \frac{4\pi}{3AR_0^2} \sqrt{\langle Q_{20} \rangle + 2 \langle Q_{22} \rangle}$  with  $R_0 = 1.2A^{1/3}$  and  $\tan \gamma = \frac{\sqrt{2}\langle Q_{22} \rangle}{\langle Q_{20} \rangle}$  [41].



# Moments of inertia

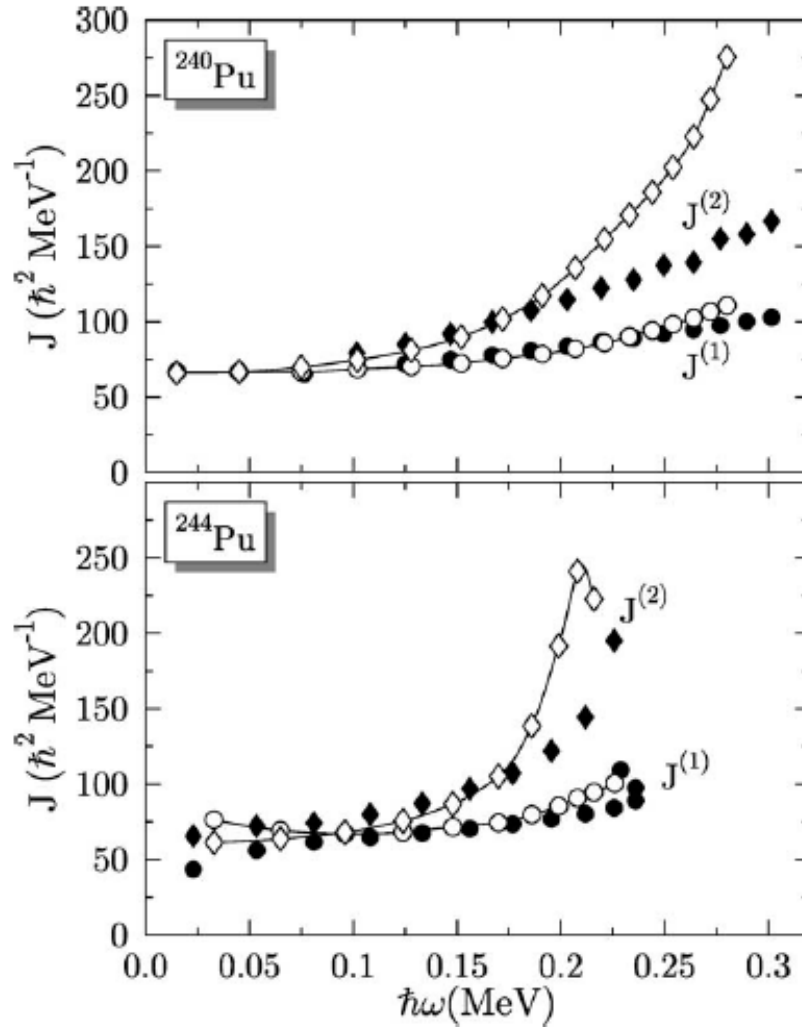


Fig. 3. Kinematical (circles) and dynamical (diamonds) moment of inertia for  $^{240}\text{Pu}$  (top) and  $^{244}\text{Pu}$  (bottom). Open (filled) markers denote calculated (experimental) values.



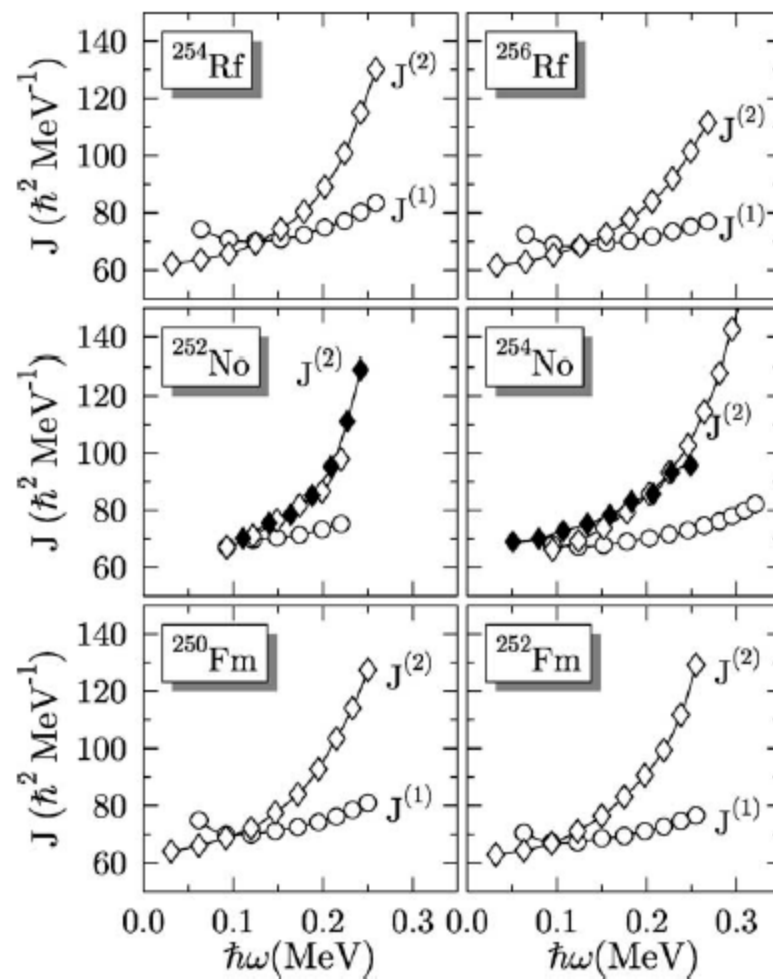
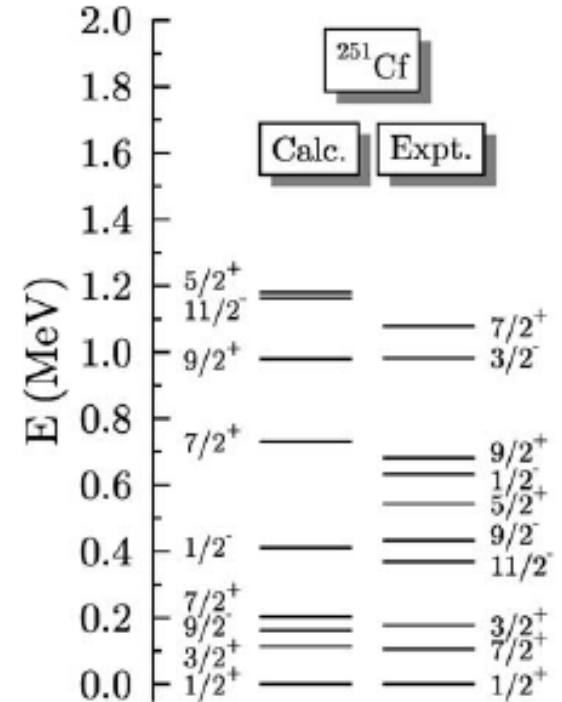
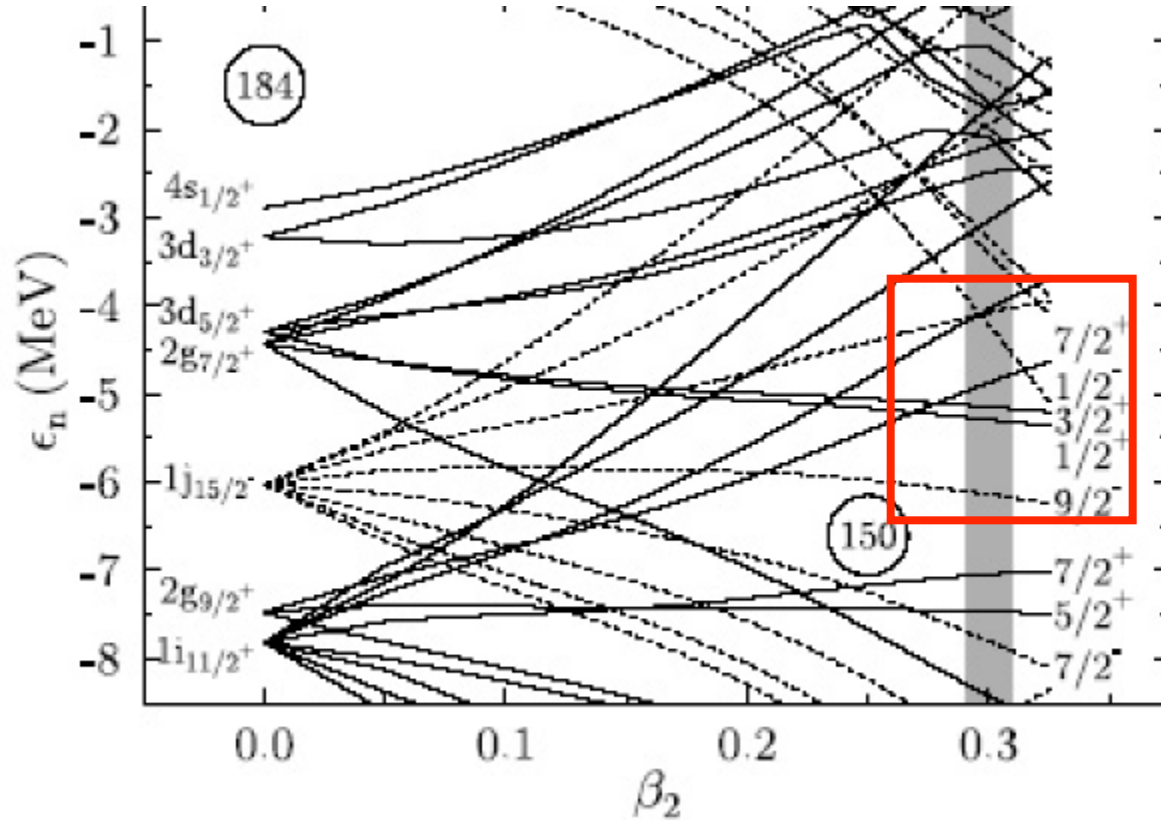


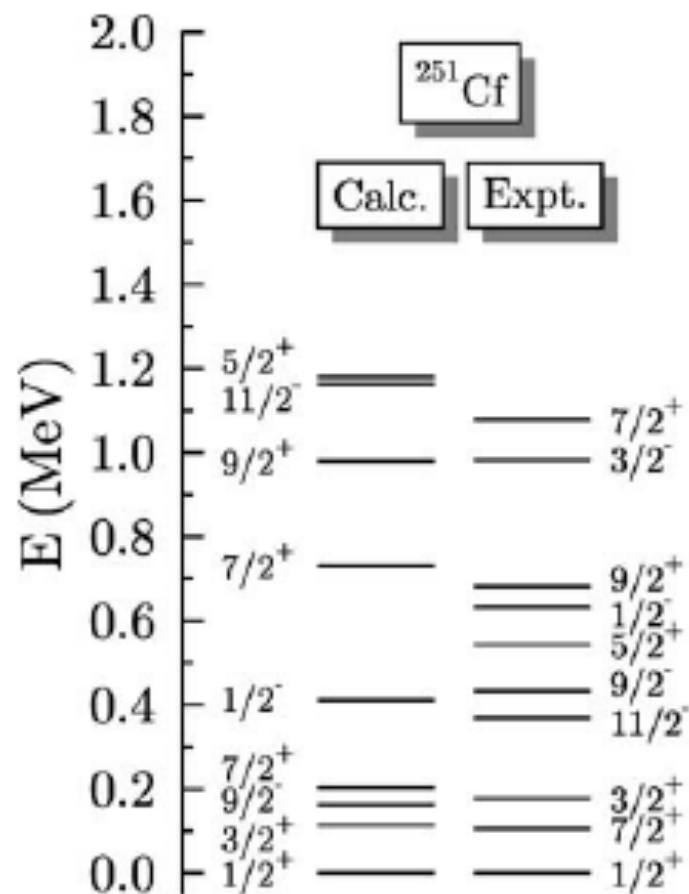
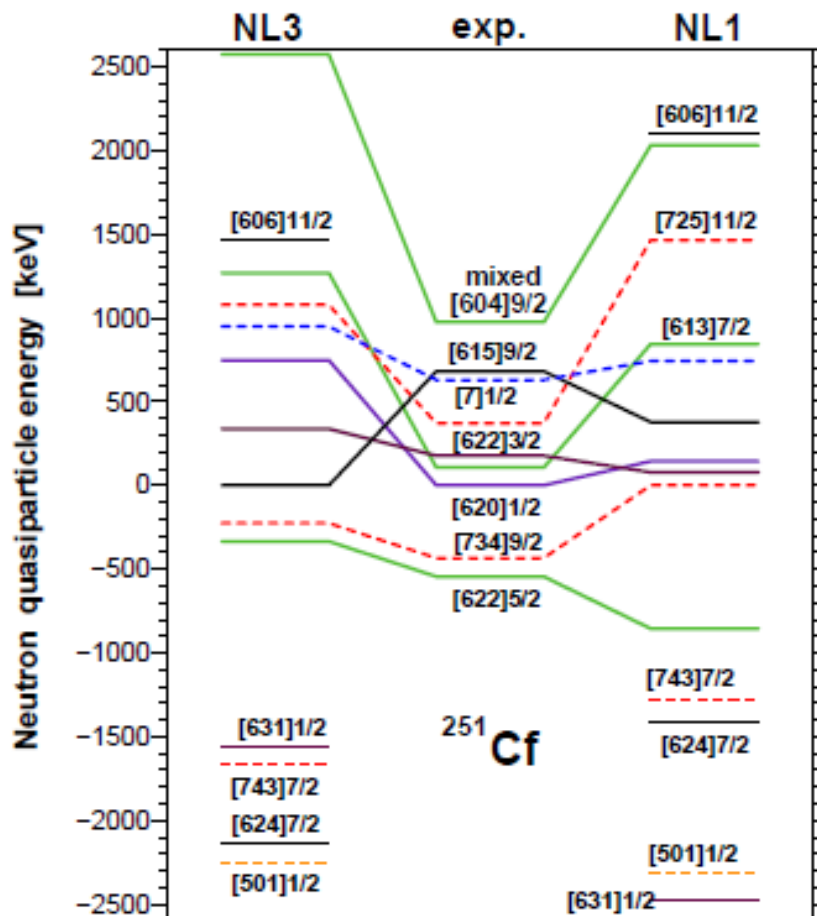
Fig. 5. Calculated kinematic,  $J^{(1)}$ , and dynamic,  $J^{(2)}$ , moments of inertia for nuclides with  $Z = 100-104$  and  $N = 150, 152$ . Empty symbols are for calculations, full ones for experiment.

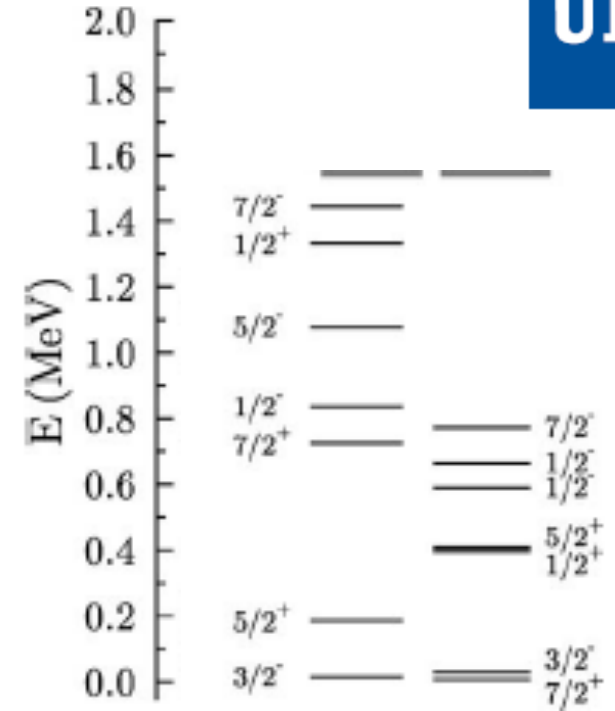
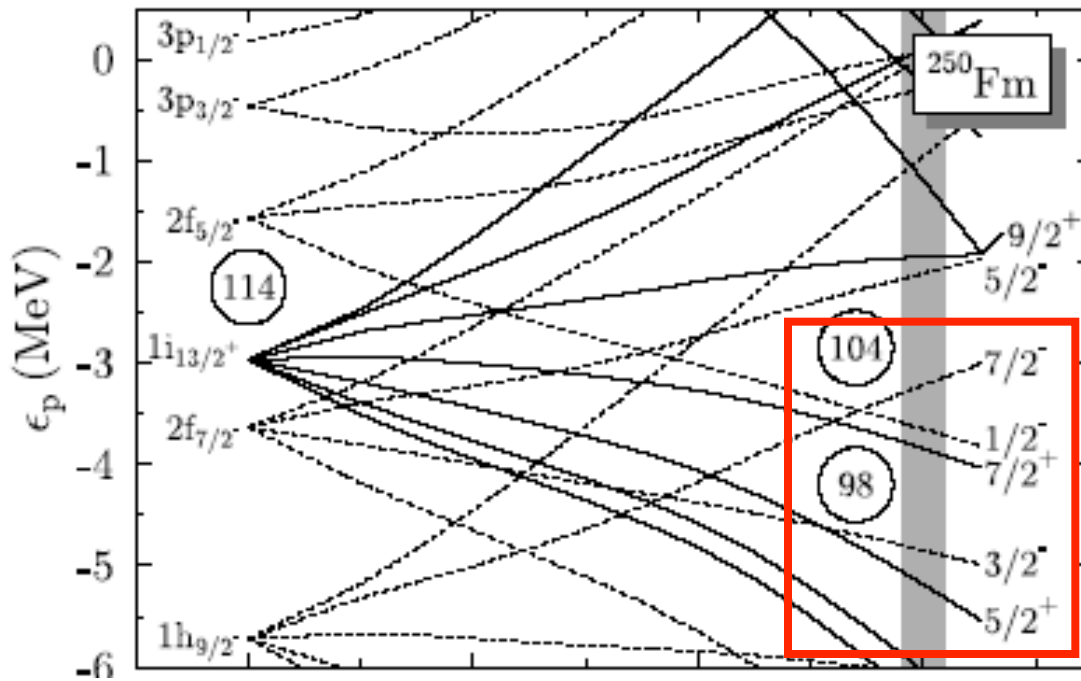
$$\beta_2^P = \sqrt{\frac{5}{16\pi} \frac{4\pi}{3R^2Z}} Q_2^P,$$



$^{251}\text{Cf}$   $Z=98$   $N=153$

Too low  $9/2^+$  and too high  $11/2^+$ : could be corrected by lowering  $1j_{15/2^+}$





$^{249}\text{Bk}$   $N= 102$   $Z= 97$

$5/2^+$  and  $7/2^+$  improved if  $j_{13/2^+}$  lower  
 $1/2^-$  and  $3/2^-$  closer if  $f_{7/2^-}$  and  $f_{5/2^-}$  closer



## Effective mass of the EDF

Constrained to be around 0.7 m in SLyX EDF's

Very low in RMF Lagrangians (around 0.6m)

An increase of the effective masse -> more dense spectrum  
(based on Mahaux et al. in the 80's , correlations increase the effective mass)

Pure WS -> effective mass = nucleon mass  
(not the case in Chasman WS!)

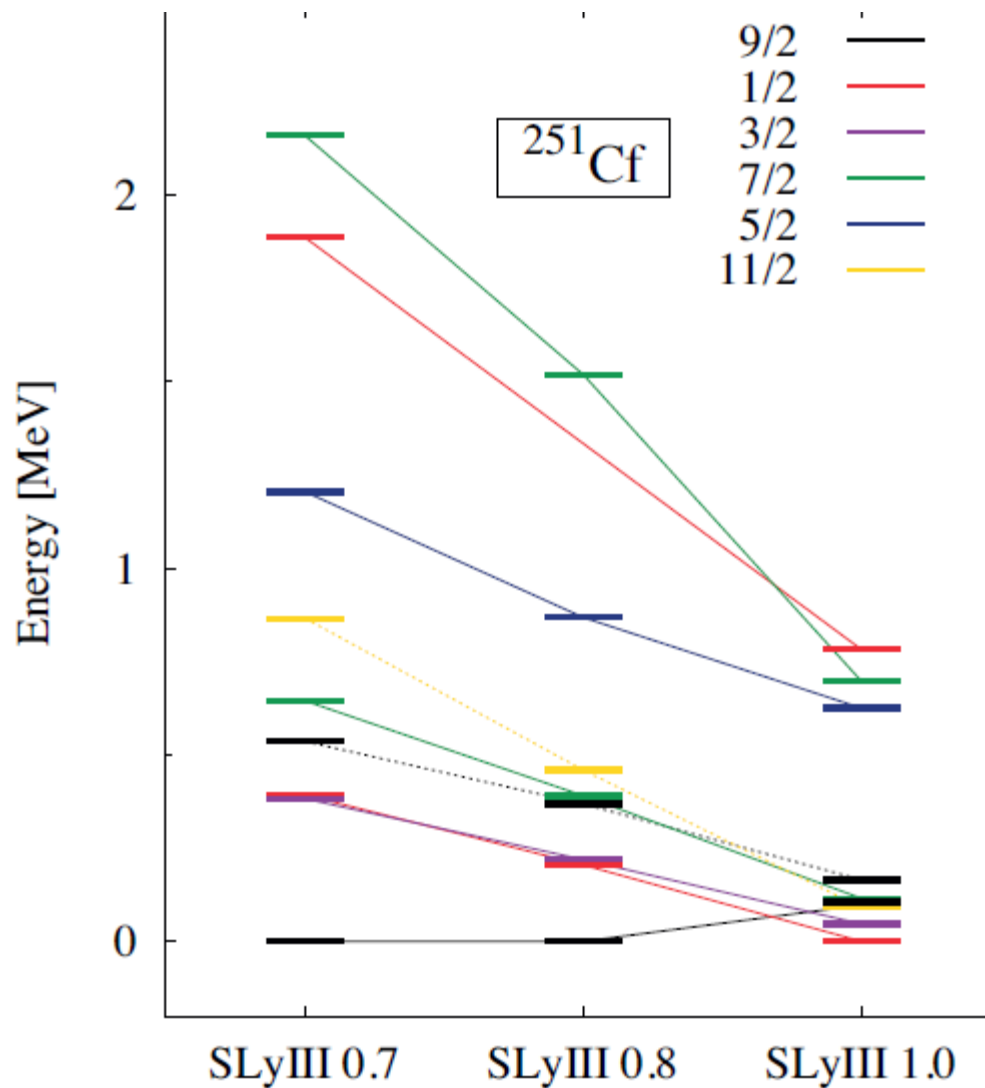
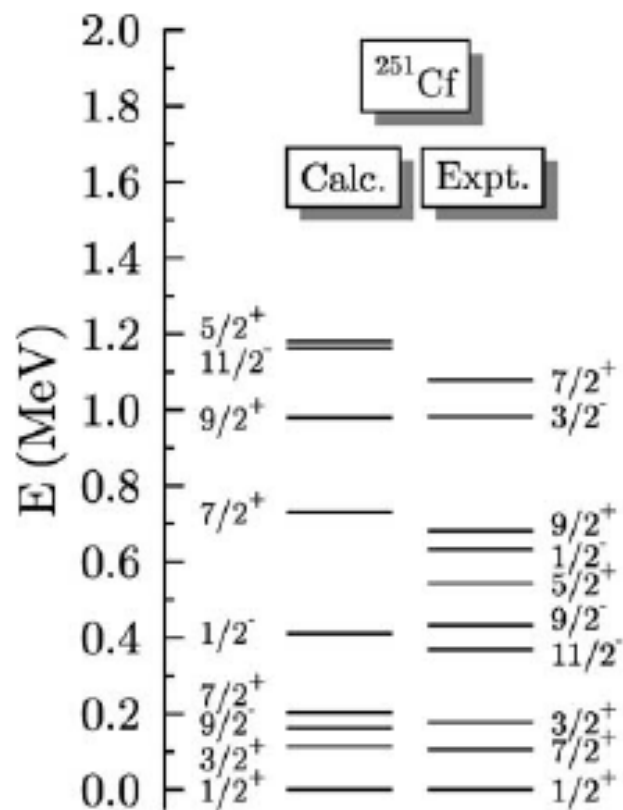
## Caution!

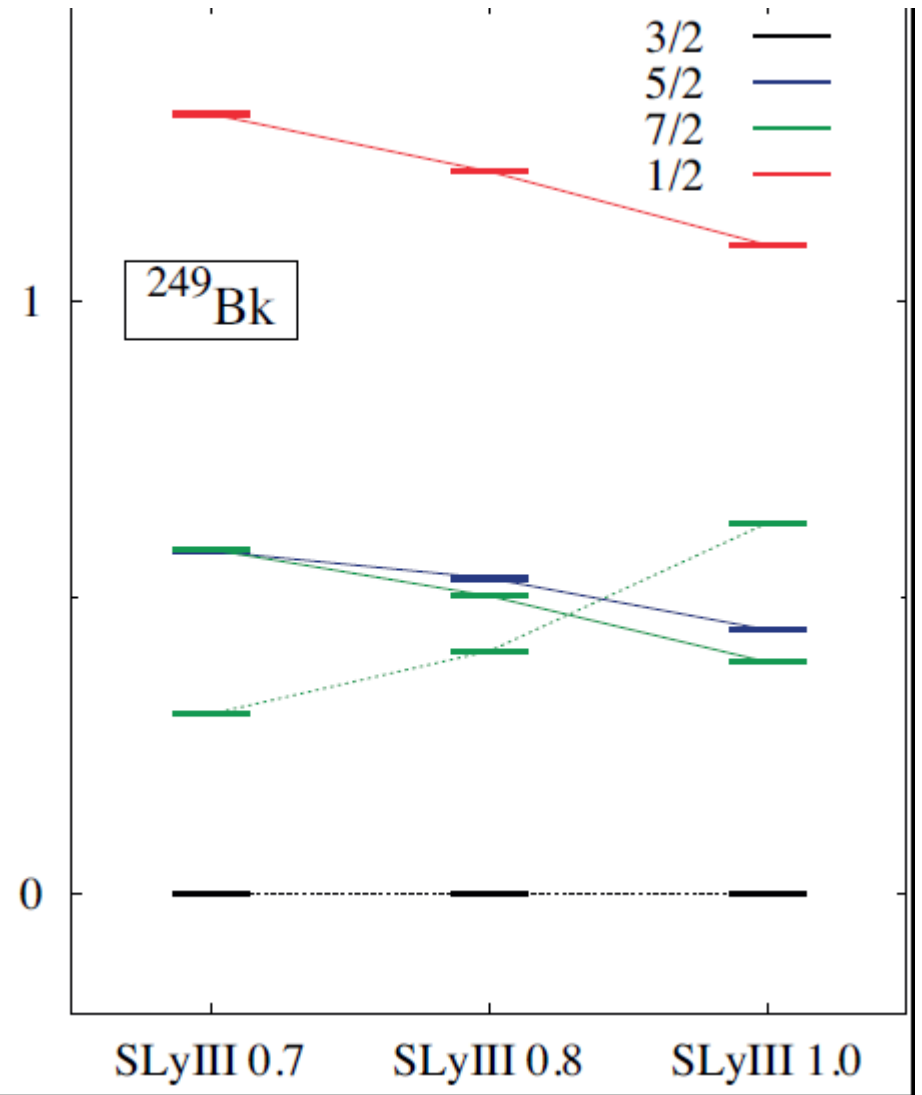
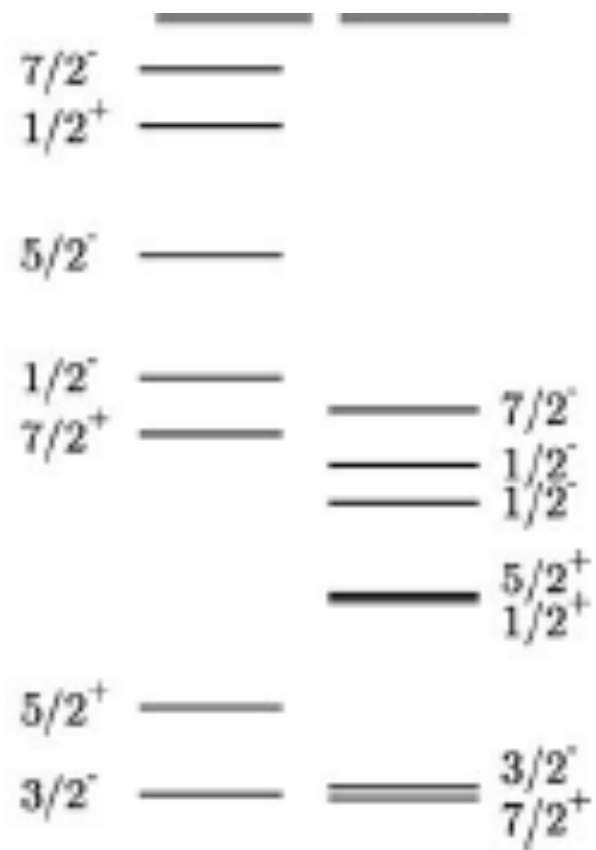
The effect of the effective can be drawn without ambiguity only for parameterizations that have been adjusted in the same way.

SLIII family : improvement of SIII by a fitting protocol similar to the Sly's

- with inclusion of deformation properties of selected nuclei
- an exponent for the density dependence equal to 1  
(to avoid some problems in beyond mean-field calculations)

$\alpha = 1$  -> compressibility of infinite nuclear matter cannot be right  
effective mass can be varied (K and  $m^*$  strongly linked)







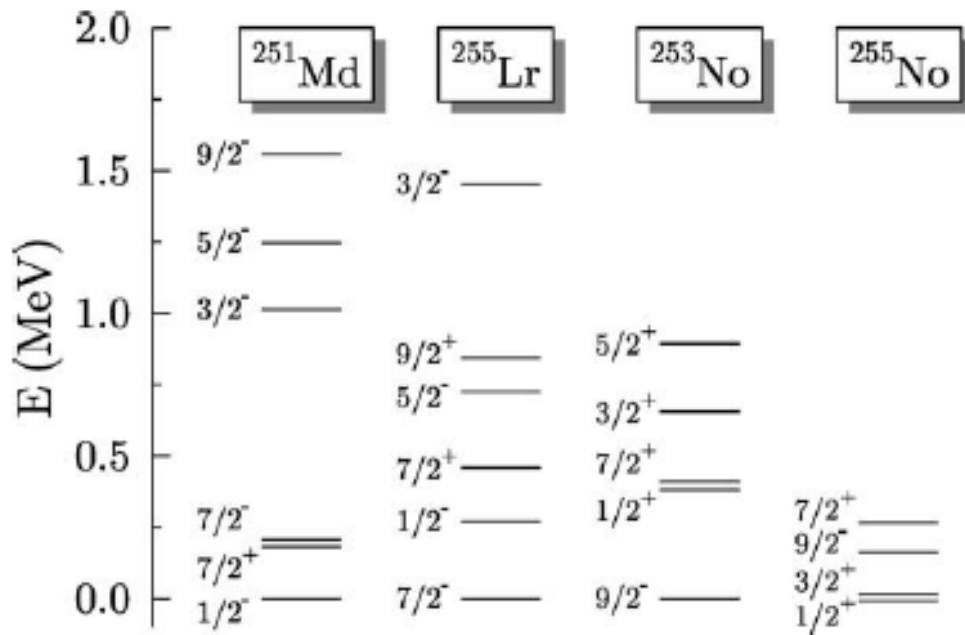
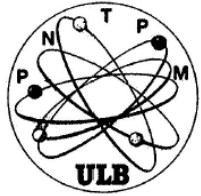
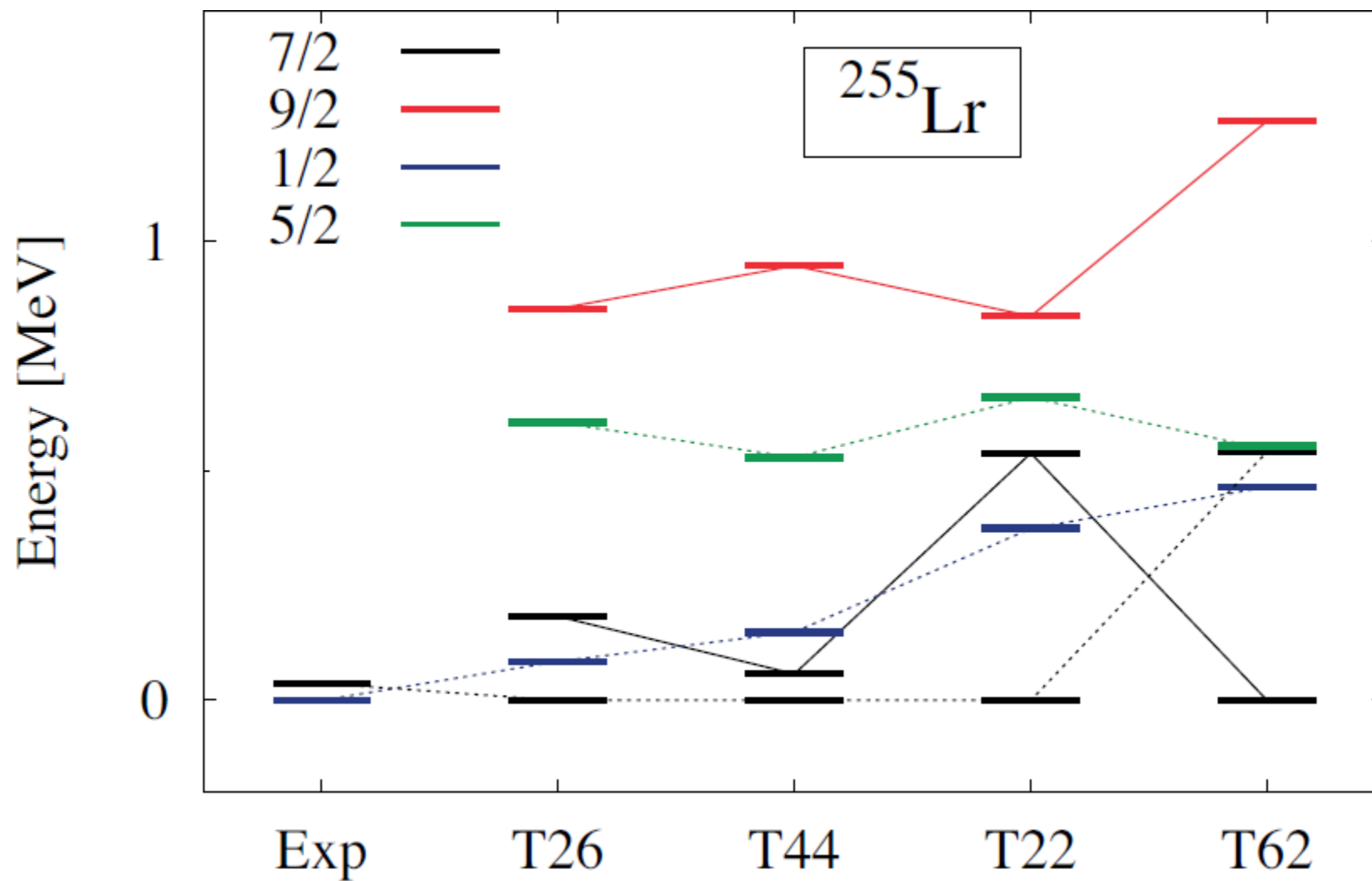
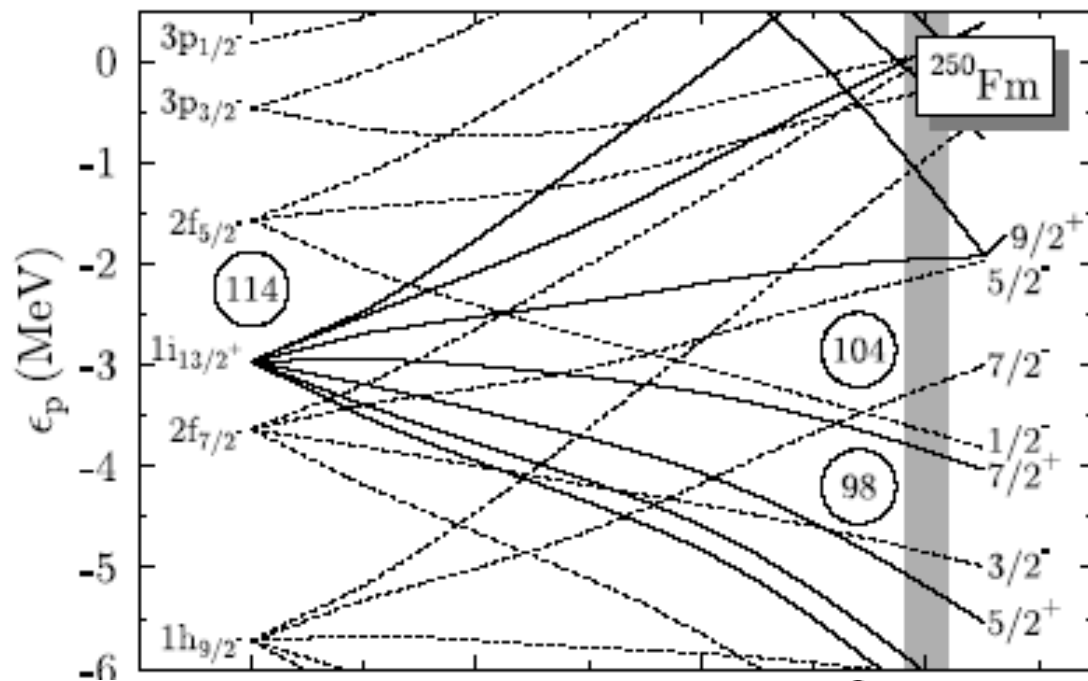
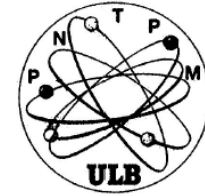


Fig. 4. Low lying energy spectra of  $^{251}_{101}\text{Md}$ ,  $^{255}_{103}\text{Lr}$  (odd Z),  $^{253}_{102}\text{No}_{151}$ , and  $^{255}_{102}\text{No}_{153}$  (odd N).

Has a tensor term in the EDF an effect on spectra?





$Z = 99, 101, 103$

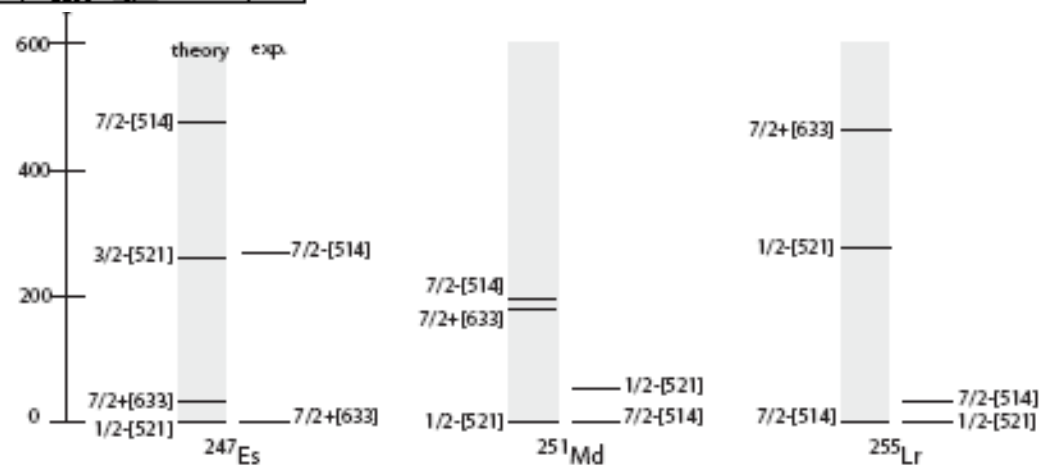


Fig. 12. Comparison between experimental and theoretical level schemes for  $^{247}\text{Es}$ ,  $^{251}\text{Md}$  and  $^{255}\text{Lr}$ .

Careful analysis of RMF results leads to similar conclusions: some orbitals are not placed as they should to reproduce experimental spectra with an accuracy better than 500 keV

The lowering of  $n j_{15/2}$  and  $p i_{13/2}$  can be done by increased spin orbit but not consistent with other analyses.

Changes of spherical gaps would change the deformed  $Z=110$  and  $Z=108$  deformed gaps. Probably not much effects on  $Z=114$

# Conclusions

Full HFB calculations can be systematically done for SHE nuclei

Global properties (deformation,  $\alpha$  decay energies, ...) correctly described

Beyond mean-field methods should be applicable in a few years  
(projection, configuration mixing): particle-vibration coupling

The tool needed to improve the description of 1qp (and 2qp!) states has still to be found.